Cyclical DNA methyltransferase 3a expression is a seasonal and oestrus timer in reproductive tissues.

Eloise WJ Lynch, Chris S Coyle, Marlene Lorgen, Ewan M Campbell, Alan S Bowman & Tyler J Stevenson*

Institute for Biological and Environmental Sciences, University of Aberdeen, Aberdeen, UK

Abbreviated title: Epigenetic plasticity in peripheral reproductive tissues

Key terms: fertility, oestrogen, melatonin, season, oestrus

Word count: 6392

Number of figures: 7
Supplementary material: 4

**Corresponding author:*
Tyler J Stevenson
Institute for Biological and Environmental Sciences
University of Aberdeen
Aberdeen, UK
AB24 2TZ
Email: tyler.stevenson@abdn.ac.uk

Disclosure statement: The authors have nothing to declare

Abstract

It is becoming clear that epigenetic modifications such as DNA methylation can be dynamic and in many cases, reversible. Here, we investigated the photoperiod and hormone regulation of DNA methylation in testes, ovaries and uterine tissue across multiple time scales. We hypothesized that DNA methyltransferase 3a (*dnmt3a*) is driven by photoperiodic treatment, exhibits natural variation across the female reproductive cycle and that melatonin increases whereas estrogen reduces DNA methylation. We used Siberian hamsters (*Phodopus sungorus*) due to their robust changes in reproductive physiology across seasonal and oestrus time scales. Our findings indicate that short day (SD) – winter like conditions significantly increased global DNA methylation and *dnmt3a* expression in the testes. Using immunohistochemistry, we confirm that increased *dnmt3a* expression was primarily localized to spermatogonium. Conversely, the ovaries did not exhibit variation in DNA methylation or *dnmt3a/3b* expression. However, exposure to SD significantly increased uterine *dnmt3a* expression. We then determined that *dnmt3a* was significantly decreased during the oestrus stage. Next, we ovariectomized females and subsequently identified that a single estrogen+progesterone injection was sufficient to rapidly inhibit *dnmt3a* and *dnmt3b* expression. Finally, we demonstrate that treatment of HEK293 cells with melatonin significantly increased both *dnmt3a* and *dnmt3b* expression suggesting that long-duration nocturnal signalling in SD may be involved in the regulation of DNA methylation in both sexes. Overall, our data indicate that *dnmt3a* shows marked photoperiod and oestrus plasticity that likely has broad downstream effects on the timing of the genomic control of reproductive function.

Introduction

Biological rhythms in reproductive physiology are common across vertebrates; from fish and reptiles to bird and mammalian species (1-3). Our understanding of a role for epigenetic modifications, such as DNA methylation, in regulating biological rhythms is in its infancy. Daily rhythms in metabolism and food intake are strongly associated with cyclical changes in histone acetylation (4,5). Moreover, daily changes in the amount of DNA methylation in a number of gene promoter regions are involved in timing circadian locomotor behavior (6). Despite these advances, the role of epigenetic rhythms during reproductive cycles is not well described. In seasonally breeding species such as the Siberian hamster (*Phodopus sungorus*), the hypothalamus exhibits photoperiod-dependent reduction in global DNA methylation and enzymes involved in the methylation of DNA (7). Whether similar changes in DNA methylation occur in the timing of reproductive physiology in peripheral tissues, such as the testes, ovary and/or uterus, is poorly understood.

In mammals, the key enzymes that catalyze the methylation of DNA consist of three distinct isoforms: DNA methyltransferase 1 (*dnmt1*), 3a (*dnmt3a*) and 3b (*dnmt3b*). *dnmt1* is critical for maintenance methylation of DNA during cell division; whereas both *dnmt3a* and *dnmt3b* are involved in *de novo* methylation primarily in post-meiotic cells (8,9). *dnmt1, 3a* and *3b* enzymes have been identified in testes, ovary and uterine tissue. *dnmt1, dnmt3a* and *dnmt3b* are predominantly localized in the spermatogonia (10), epithelial layer in ovaries (11) and endometrium cells in the uterus (12). The localization of *dnmts* in peripheral reproductive tissues indicates the potential for timing cyclical changes within molecular pathways involved in fertility (13). Indeed the mechanisms that regulate the functional role of methyltransferases are well described in germline cells and during development (reviewed by 14). The objective of this paper was to examine photoperiod and hormone dependent changes in DNA methylation and *dnmt1, dnmt3a* and *dnmt3b* mRNA expression in adult testes, ovary and uterine tissues.

Given the massive seasonal and oestrus changes in testicular and uterine tissue in Siberian hamsters, we tested the hypotheses that peripheral reproductive tissues exhibit significant variation in global gonadal DNA methylation and DNA methyltransferase expression. Here, we investigated the photoperiod and hormonal regulation of gonadal DNA methylation and *dnmt1, dnmt3a* and *dnmt3b* expression in testicular, ovarian and uterine tissue and cell culture. Using adult male and female Siberian hamsters, we identified marked naturally

occurring plasticity in *dnmt3a* methyltransferase expression that is regulated by photoperiod, melatonin and ovarian hormones. Increased *dnmt3a* in short day (SD) testes results in a substantial accumulation of global DNA methylation. The findings reported herein reveal robust plasticity in key DNA methylation enzymes and indicated epigenetic reorganization within peripheral reproductive tissues across multiple time scales. Overall, this work has significant implications for reproductive timing and fertility in mammalian species.

Methods

Animals

Adult male and female Siberian hamsters (Total N=100; 3-8 month old) were randomly selected from a colony maintained at the University of Aberdeen. Adulthood in hamsters occurs between the age of 3-9m months (15). Hamsters are classified as aged at 14 months (16) and reproductive decline does not occur in females until after 9 months (15). Hamsters were housed in polypropylene cages in a long day (LD) photoperiod (15L:9D). Food and water were provided *ad libitum* and hamsters were provided cotton-nesting material. All procedures were approved by the Animal Welfare and Ethics Review Board at the University of Aberdeen and conducted under the Home Office licence (70/7917).

Experimental designs

Photoperiod regulation of reproductive physiology and gonadal DNA methylation

Thirty-six adult male and female hamsters (3-8 months) were used in this study. Male (n=8) and female (n=8) hamsters were group housed in long day (15L:9D) conditions prior to the experiment. Baseline measures of body weight were recorded and measured for the duration of the experiment. A group of males (n=10) and females (n=10) were transferred from LD to short day cabinets (Arrowmight; SD 9D:15L) for 8 weeks. At the termination of the study animals were sacrificed by cervical dislocation and testes, ovary and uterine mass was determined using aeADAM scales (Adam Equipment PGL2002) and measured to ±0.1g. Tissues were frozen in powdered dry ice and stored at -80°C until global gonadal DNA methylation and RNA expression analyses (see below).

Naturally occurring changes in uterine DNA methyltransferase enzymes across the oestrus cycle

Female hamsters (N=33) were group housed and maintained in LD. On the final day of the experiment, animals were sacrificed from 1500-1700 in order to capture the proestrus surge in prolactin (17). Females were lightly anaesthetized with isofluorane gas (4%) and 500 µl whole blood was collected via the right retro-orbital sinus using Natelson tubes coated with sodium heparin. The blood samples were kept on ice and then centrifuged at 9000rpm (3622g) in 4°C for 20 minutes. Plasma was removed and stored at -20°C until prolactin levels were determined by ELISA assay (see below). Females were sacrificed by cervical dislocation and uterine mass was measured and subsequently frozen in powdered dry ice. Samples were kept at -80°C until RNA extraction.

Unlike mice and rats, female hamsters do not exhibit marked cyclical changes in vaginal cell types resulting in the inability for external tracking of the oestrus stages. In order to determine stage of oestrus cycle we took advantage of a well described method that uses convergent measures consisting of uterine mass and plasma prolactin concentrations (17). The combinations of reproductive measures permit the identification of diestrus (low prolactin; small uteri), proestrus (high prolactin; intermediate uteri) and oestrus (low prolactin; engorged uteri) stages of the female cycle. Plasma prolactin concentrations were determined using a Hamster Prolactin ELISA (2BScientific Ltd, Oxfordshire, UK). Samples were assayed in duplicate and compared to a standard curve. The intra-assay coefficient was 4.4%. Analyses of the uterine weight and plasma prolactin values resulted in the identification of diestrus (n=13), proestrus (n=12) and oestrus (n=8) females.

The sufficiency of ovarian steroids to regulate DNA methylation enzymes

In order to assess the sufficiency of ovarian hormones on uterine DNA methyltransferase expression, females were ovariectomized (N=21) and maintained in LD for 8 weeks to reduce circulating levels of gonadal steroids. In brief, ovariectomies were conducted while hamsters were under deep anaesthesia (5% isofluorane gas). The ovaries are externalized via bilateral incisions to the dorsum (lateral to the spine, caudal to the ribcage). The ovary was localized at the distal end of the uterine horn and ligated with sterile sutures (4-0, non-absorbable monofilament nylon). The ovary was then excised and repeated for the other ovary. The abdominal wall and skin were closed separately with sterile sutures (5-0 non- absorbable and 4-0 non-absorbable, respectively; monofilament nylon). After ovariectomy, female body mass decreased on average 7.5g (±0.9

SEM); a reliable long term indicator of reduced ovarian steroids (18). Estrogen and progesterone (E2P4) injections were prepared by dissolving diethylstilbestrol (Sigma Aldrich, UK) and progesterone (Sigma Aldrich, UK) in sterile vegetable oil to a final concentration of 5µg E2 and 500µg P4 in 100µL vegetable oil (OIL). These values were selected based on previous work in female hamsters (19). Females received an intraperitoneal injection at 1700 with 100µl of the hormone cocktail. Control hamsters were injected with 100µl of OIL. The following day hamsters were sacrificed at 12h (n=6) and 24h (n=6) post-injection by cervical dislocation and uterine weights were measured and frozen in powdered dry ice. We selected 12hr and 24hr time points to control for potential daily variation in *dnmt3a* or *dnmt3b* expression. OIL controls were counterbalanced across the 12h and 24h collection periods.

Assessment of global gonadal DNA methylation

DNA was extracted from tissues using DNeasy kits (QIAGEN, UK) following the manufacturer's directions. 1µg of DNA was digested using nuclease P1 (5 units; Sigma Aldrich, UK) and then incubated at 70ºC for 30 minutes. 1 µl of alkaline phosphatase (5 units; Sigma Aldrich, UK) was added and the samples were incubated at 37ºC for 30 minutes. The samples were then transferred to 65ºC for 15 min and then placed at -20ºC until assayed. Global DNA methylation levels were measured using a 5'-methyl-2'-deoxycytidine quantitation ELISA kit (Cell Biolabs Inc.). The kit is a competitive assay used for the quantification of 5-methyl-2'-deoxycytidine and has previously been used in Siberian hamsters (7). Samples were run in duplicates and the intra-assay CV was 10%.

Quantification of RNA expression

RNA was extracted from tissues using Trizol (ThermoFisher Scientific). Nucleic acid concentration and quality were determined by spectrophotometer (Nanodrop, Thermo Scientific). cDNA was synthesized using Superscript III (Invitrogen) and cDNA was stored at -20ºC until quantitative PCR was performed. All cDNA tissue samples were run in triplicate; cDNA from HEK293 cell culture and oestrus study were assayed in duplicate. qPCRs were performed using a BIORAD CFX96 system using the following steps i) an initial denature at 95°C for 30 secs, then 39 cycles of ii) 95°C for 10 sec, iii) annealing dependent on target mRNA

(See Table S1) for 30 secs and then iv) an extension at 72°C for 30 sec. The specificity of select samples was established by resolving PCR products in 2.5% agarose gel. A melting curve analysis was added to determine the quality and specificity of each reaction. Quantification of mRNA expression levels was accomplished with iQ Sybr Green Supermix (BIORAD, UK). We used PCR Miner (22) to calculate reaction efficiencies (E) and cycle thresholds (CTs). According to the MIQE guidelines, samples that had efficiency values below 0.8 or above 1.2 were excluded from analyses (23). The expression of each target gene of interest was measured in relation the average cycling time (CT) for two reference targets: glyceraldehyde 3-phosphate dehydrogenase (*gapdh* 7,24) and 18S ribosomal RNA (*18s; 25*) and calculated using 2-(delta-deltaCt).

Histological analyses of dnmt3a

Male hamsters (n=10) were divided into LD and SD conditions (n=5 each) for 8 weeks. Testes length and width were measured, weighed and frozen in powdered dry ice. Testes were sectioned at 30 µm with a cryostat (Reichert-Jung) in series of three. Microscope slides were then placed at -80°C until the immunocytochemistry (ICC) procedure. Testes sections were washed three times for 5 minutes in 0.1% tween-20 (Sigma-aldrich) in 1M PBS (PBSt). Then tissues were incubated in 3% hydrogen peroxide for 20 minutes followed by three 5 minute washes in PBSt. Tissues were incubated in 10nM sodium citrate at 83ºC for 30 minutes followed by three 5 minute washes. Tissues were then incubated in 5% normal goat serum for 1 h at room temperature, and then with the DNMT3a primary antibody (PA3-16557, ThermoFisher) at 4ºC for 48 hours. The sections were then washed 3 times, incubated in a biotinyated goat anti-rabbit second antibody (Vector Labs) for 1 h at room temperature, washed 3 times, incubated in avidin biotin horseradish peroxidase complex (Vectastain ABC Elite, 1:200) for 1 h, and then washed 3 times. DNMT3a was visualized by incubating tissue sections in fluorescein (Vector Labs) for 5 minutes. Sections were then washed 3 times, serially dehydrated and cover slipped using Vectashield mounting medium with DAPI (Vector Labs). Sections were examined using fluorescence light microscopy (Zeiss), and photomicrographs were captured using Zeiss Slide scanner AxioScan.Z1. Photomicrographs were analysed using ImageJ and cell counts were conducted using unbiased stereology (26) as previously described (27). The number of DNMT3a cells determined taking the sum of immunoreactive cells from 10 randomly selected seminiferous tubules for each hamster.

The specificity of the ICC signal was tested using four controls. We conducted the ICC protocol in the absence of the primary antibody, no secondary antibody and no fluorescein. In all cases, the immunoreactivity signal was abolished. Preadsorption of the primary antibody with 5ug or 10ug blocking peptide (3227BP; Cambridge Bioscience Ltd) for 2 hours resulted in a dose-dependent decrease in staining intensity ($p<0.05$ and $p<0.001$, respectively). Overall, these data indicate that the primary antibody used here is specific for the endogenous DNMT3a antigen.

Sufficiency of melatonin to drive DNA methylation enzymes

In order to assess the potential direct effects of melatonin on *dnmt3a* and *dnmt3b* expression, we conducted a melatonin dose-dependent study using cell culture. Given the low levels of DNA methylation and absence of *dnmt3a/3b* plasticity in the ovary (see results below) we selected HEK293 to examine the role of melatonin dependent regulation of *dnmt* expression as these cells are known to express melatonin receptor 1a (28). Cells of the HEK293 cell line were grown in Dulbecco's modified eagle's medium (DMEM) supplemented with 10% Fetal bovine serum, 1% Penicillin/Streptomycin and sodium pyruvate (complete medium) in a T75 flask in a humidified atmosphere at 37°C with 5% CO_2. HEK293 cells were selected for melatonin assay as these cells express *dnmt3a* and *dnmt3b* as well as the melatonin receptor involved in the neural control of the seasonal photoperiodic response (20,21). When confluent, HEK293 cells were plated in 24 well plates as follows. Media was removed and cells were rinsed with Phosphate buffered saline (PBS at 37°C) and 5ml of trypsin was added to detach cells. 2ml of media was added before pipetting up and down to mix and transferring to a 15ml tube to pellet cells by centrifugation. Supernatant was removed and cells re-suspended in 7ml complete medium (at 37°C). 150µl of cell suspension (~$1x10^6$ cells) was added to each well in a total volume of 1.5ml complete medium. Cells were allowed to settle for 48 hours in a humidified atmosphere at 37°C with 5% CO_2 before stimulation. In order to examine the sufficiency of melatonin (Sigma Aldrich, UK) to induce RNA expression, HEK93 cells were assigned to four treatment groups: (1) saline controls; (2) 1nM melatonin (3) 10nM melatonin or (4) 100nM melatonin. Stimulated cells were incubated for 4 hours in a humidified atmosphere at 37°C with 5% CO_2. Wells containing cells and medium were then transferred to -80°C.

Statistical analyses

SigmaStat 13.0 was used for all statistical analyses and significance was determined at $p < 0.05$. Shapiro-Wilk Normality tests were conducted on all data sets to ascertain whether parametric or non-parametric analyses were appropriate. T-test was conducted to examine photoperiod effects on testes, ovarian and uterine mass as well as global DNA methylation and DNA methyltransferase expression. One-way ANOVA was conducted to examine the effect of hormone (i.e. E2P4, melatonin) treatment on *dnmt* expression. Dunnett's *post hoc* analyses were performed to compare hormone treatment versus untreated control conditions. Fishers Least Square Difference (LSD) was conducted to determine significant difference in uterine mass, plasma prolactin concentrations and *dnmt* expression across the oestrus cycle. Log-transformation was conducted on qPCR data when violations in normality were detected.

Results

SD induced gonadal involution facilitated testicular DNA methylation

Exposure to SD significantly reduced testes mass (t=14.33; p<0.001; Fig1a). Regressed testes were observed to have a robust and significant effect on global DNA methylation levels (t=3.17; p<0.005; Fig1b); indicating that the timing of testicular involution may be controlled by increased DNA methylation. Next, we assessed the levels of DNA methyltransferase expression in order to identify the enzymes involved in the catabolism of increased DNA methylation in regressed testes. *dnmt1* expression was found to have significantly greater levels in LD compared to SD conditions (t=2.77; p<0.01; Fig S1a). Increased *dnmt1* in LD testes may be due to the production of sperm during the breeding periods. *dnmt3a* expression was observed to exhibit the predicted increase in SD testes, regressed testes had significantly greater levels compared to LD (t=2.80; p<0.01; Fig1c). *dnmt3b* expression was found to remain constant across photoperiodic conditions (t=0.79; p=0.22; Fig1d).

Regressed testes have more DNMT3a expressing cells

A *t*-test was conducted to evaluate the effect of SD on the number of DNMT3a expressing cells in the testes. SD significantly reduced testes mass (t=9.05; p<0.001; Fig2a). There was a significant increase in the

number of DNMT3a cells in the SD compared to LD testes (t=2.159; p<0.05; Fig 2b-d). The SD increase in DNMT3a appears to be localized to spermatogonium (Fig S2).

Ovarian DNA methylation remains constant across photoperiodic conditions.

Ovary mass showed a relatively small, yet significant decrease in SD compared to LD hamsters (t=2.17; p<0.05; Fig3a). Unlike the testes, there was no significant photoperiodic effect on ovarian global DNA methylation (t=0.81; p=0.21; Fig3b). Not surprisingly, there was no significant difference between LD and SD levels of *dnmt1* (t=1.39; p=0.09; FigS1b), *dnmt3a* (t=0.27; p=0.39; Fig3c) or *dnmt3b* expression (t=0.62; p<0.27; Fig3d).

SD significantly increased uterine dnmt3a and dnmt3b

Exposure to SD significantly reduced uterine mass (t=3.388; P<0.005; Fig4a). Photoperiodic condition did not significant effect on *dnmt1* expression (t=0.95; p<0.18; FigS1c). The decrease in uterine mass was paralleled by a significant increase in *dnmt3a* expression (t=3.103; P<0.05; Fig4b) and *dnmt3b* expression (t=10.0; P<0.01; Fig4c). Histological analyses indicate that DNMT3a expression in SD shows a robust immunoreactive signal in the endometrium layer in the uterus (12, FigS3).

dnmt3a expression is reduced during oestrus

As previously established (Dodge *et al*., 2002), the oestrus cycle in female hamsters can be determined using the combined uterine mass and plasma prolactin measures. A one-way ANOVA indicated that uterine mass exhibits significant variation across the cycle (F=15.623; P<0.001; Fig5a). LSD *post-hoc* analyses confirmed that diestrus females have significantly lower uterine mass compared to proestrus (P<0.01) and oestrus (P<0.001) stages. Furthermore, the uterine mass during oestrus was significantly engorged and greater compared to proestrus (P<0.005). Plasma prolactin exhibited significant variation across the oestrus cycle (F=24.202; P<0.001; Fig5a). LSD analyses indicated that plasma prolactin concentrations significantly increased from diestrus to proestrus (P<0.001). Plasma prolactin concentrations then decreased during the oestrus phase (P<0.001). Oestrus females were found to have slightly higher levels of plasma prolactin compared to diestrus females (P<0.05).

A one-way ANOVA revealed a significant difference in *dnmt3a* (F=3.53; P<0.05; Fig5b) expression across the oestrus cycle. LSD analyses indicated that *dnmt3a* expression significantly decreased during the

transition from proestrus to oestrus (P=0.01). Diestrus females had intermediate levels as *dnmt3a* levels were not significantly different compared to oestrus (P=0.44) or proestrus (P=0.06) hamsters. There was no significant variation in *dnmt3b* expression observed across diestrus, proestrus or oestrus phases (F=2.22; P=0.33; Fig5c). There was no significant change in *dnmt1* expression across the oestrus cycle (F=0.26; P=0.77; FigS1d).

E2P4 is sufficient to inhibit DNA methyltransferase expression

Kruskal-Wallis ANOVA revealed that a single bolus injection of E2P4 was sufficient to significantly increase uterine mass (H=8.34; p<0.05; Fig6a). Dunnett's method identified that uterine mass was significantly greater than OIL treated controls 12hr (p<0.05) and 24hrs (p<0.05) post-injection. These data confirm that E2P4 was capable of inducing engorged uterine and oestrus within 24hrs. A one-way ANOVA revealed a significant difference in *dnmt3a* expression after administration of E2P4 (F=13.57; P<0.001; Fig6b). Dunnett's Method indicated that E2P4 induced a rapid inhibition in *dnmt3a* expression with a significant reduction after 12hr (P<0.001) and 24hr (P<0.001) compared to OIL treated females. Similarly, there was a significant difference in *dnmt3b* across treatment groups (F=32.35; P<0.001; Fig6c). E2P4 significantly reduced *dnmt3b* expression in uterine tissue 12hr (P<0.001) and 24hrs (P<0.001) after administration. *dnmt1* expression was also found to be significantly reduced by E2P4 treatment (F=8.79; P<0.005; FigS1e). Dunnett's method revealed that *dnmt1* expression was significantly lower 24hr after injection (P<0.005), but not 12hrs (P=0.51).

Melatonin is sufficient to increase dnmt3a and dnmt3b

Melatonin treatments categorically increased *dnmt3a* and *dnmt3b* expression in HEK293 cells. A one-way ANOVA revealed a significant difference in *dnmt3a* expression across treatment groups (F=17.207; P<0.001; Fig7a). Dunnett's Method for *post-hoc* analyses established that all doses of melatonin induced a significant increase in *dnmt3a* compared to control cells (P<0.001), but *dnmt3a* expression was similar across all melatonin concentrations (P>0.05). Similarly, the one-way ANOVA revealed a significant difference in *dnmt3b* expression (F=39.207; P<0.001; Fig7b). All doses of melatonin were observed to have significantly greater *dnmt3b* expression compared to controls (P<0.001).

Discussion

In this paper, we show marked photoperiod dependent regulation of DNA methylation in testes. The increased methylation appears to be driven by *dnmt3a* and likely *dnmt3b,* albeit to a lesser extent. One potential driver for the short day induced increase in DNA methylation may be a lengthening of nocturnal melatonin duration. Incubation of HEK293 cells with various concentrations of melatonin was sufficient to elicit a categorical increase in both *dnmt3a* and *dnmt3b* expression. Surprisingly, the ovary failed to show photoperiodic variation in DNA methylation, indicating a marked gonadal difference in the role of DNA methylation across the seasonal reproductive cycle. Instead, seasonal variation in DNA methylation may act in the uterus for reproductive timing. Further examination of *dnmt3a* and *dnmt3b* expression revealed significant plasticity during the oestrus cycle, with inhibition during the oestrus stage due to the increased secretion of oestrogen and progesterone. We conclude that seasonal and oestrus variation in testicular and uterine *dnmt3a* expression enhanced DNA methylation, triggered reproductive involution and reduced fertility.

Cyclical patterns in epigenetic modifications are gradually being uncovered. Recent work has identified marked daily (6) and seasonal (7) changes in DNA methylation. In the hypothalamus, there is a decrease in global DNA methylation and *dnmt3b* expression in adult Siberian hamsters after prolonged exposure to SD compared to LD (7). Here we show SD stimulated an increase in DNA methylation and *dnmt3a* and *dnmt3b* expression in peripheral tissues (i.e. testes and uterus). These findings suggest that DNA methylation patterns show opposite cyclic changes in the central nervous system (7) compared to peripheral systems, such as reproductive tissue and immune cells (23). DNMT expression in the brain is widely distributed and located in several hypothalamic nuclei (7). Peripheral tissues (e.g. testes, ovary) consist of a relatively homogenous cell population compared to the complex networks and diverse cells located in the hypothalamus. The increased DNMT expression in LD hypothalamus likely reflects the outcome of multiple localized changes and not the result of a single brain region. A greater resolution of anatomically localized changes in DNMT expression in the hypothalamus will help resolve the opposite patterns observed in neuroendocrine nuclei and peripheral reproductive tissues. It is clear that melatonin and ovarian hormones are involved in the regulation of *dnmt3a* and *dnmt3b* expression. Given the categorical increase in *dnmt3a* and *dnmt3b* after exposure to melatonin and the rapid change in response to a single bolus of E2P4, it is likely that these hormones could be acting directly on promoter regions or in the recruitment of transcription binding factors. Altered hormonal regulation of cell

314 autonomous timing of DNA methylation may be one potential molecular mechanism that underlies seasonal
315 disruption in animal health (29).

316 Epigenetic modifications during gamete development are well described (30). Conditional knockout
317 *dnmt3a* mice exhibit severe reproductive deficits; males exhibit impaired spermatogenesis and lack DNA
318 methylation in parentally imprinted genomic regions (31). In females, conditional knockouts of *dnmt3a* are lethal
319 and also have an absence of DNA methylation at parentally imprinted genomic regions (31). These data support
320 a model in which *dnmt3a* signalling in males and females is vital for the generation of viable gametes and
321 ultimately, fertility. In our study, we observed relatively low levels of *dnmt3a* in testes and ovaries in LD
322 compared to non-breeding, SD conditions. The increase in *dnmt3a* expression in the regressed testes likely
323 provides an inhibitory signal that arrests spermatogenesis. Whether enhanced melatonin or reduced gonadal
324 steroids (i.e. E2P4) provide a hormonal signal that permits the greater *dnmt3a* expression requires further
325 exploration. Regardless, the molecular outcome was a massive increase in DNA methylation that results in broad
326 methylation across the entire genome resulting in reproductive involution. Given that the seasonal pattern in
327 DNA methylation occurs over multiple annual oscillations, we propose that cyclical DNA methylation in
328 reproductive tissues provides a single trigger with broad implications for the timing of gene transcription that
329 enables yearly switches in gamete development and fertility.

330 DNMT3a/b has a high enzymatic activity and can rapidly methylate cytosine residues (e.g. 3hrs; 32). In
331 this paper, we have shown that melatonin can increase *dnmt3a* and *dnmt3b* expression in cell culture within 4hrs
332 and a single bolus of E2P4 can inhibit uterine levels within 12hrs. These data indicate that key seasonal and
333 reproductive hormones can have a significant impact on *dnmt3a/b* expression and ultimately lead to a lasting-
334 effect on the epigenomic landscape. It is important to note that caution should be exercised when extrapolating
335 the melatonin-dependent increase of *dnmt3a/b* in HEK293 results to seasonal regulation of DNA methylation in
336 hamster reproductive tissues. Given the large variation in gene transcription during spermatogenesis (33);
337 seasonal and oestrus patterns in *dnmt3a* likely function to secure the inhibition of select genes leading to the
338 successful timing of RNA expression required for optimal fertility. It is likely that several other hormones with
339 links to reproduction function (e.g. leptin) will also impact the probability of *dnmt3a/b* expression. Overall, the
340 rapid and long-term effects of melatonin and ovarian steroids reveal a novel and robust effect on

methyltransferase expression and illustrate that hormone driven changes in the epigenomic landscape are probably more common than previously thought.

The comparison of ovarian and testicular DNA methylation permitted the identification of significant sex differences in the levels of *dnmt1* and *dnmt3a* expression. The higher levels of *dnmt1* expression in testes is likely attributable to gamete production (i.e. spermatogenesis; 34). Several testicular genes exhibit reversible, seasonal variation in expression and these changes are proposed to enhance fertility during the breeding periods (35). Since seasonal variations in sperm parameters are common across mammalian species, including humans, (36,37) the patterns in *dnmt1* and *dnmt3a* may represent an evolutionarily ancient molecular signalling mechanism for the timing of reproduction. A role for *dnmt1* in the timing of reproductive physiology in the uterus is less clear (FigS1). *dnmt3a* has been shown to be important for decidualization, exhibiting transient estrogen-dependent decrease (38). Similarly, we found that E2P4 significantly reduced *dnmt3a* and *dnmt3b*. The specific role of reduced *dnmt3a* during decidualization is unknown; but may permit stromal vascularity and/or glandular epithelial secretion.

In conclusion, we present novel and robust findings that *dnmt3a* expression is dynamic and propose that variation in *dnmt3a* is involved in the local timing of reproductive physiology in key tissues. These data have significant implications for our understanding of the potential effects of DNA methylation for fertility in a rodent species. One particularly important finding was the significant increase in global DNA methylation in the male testes during reproductive involution. Future work that includes alternative methods, such as chromatin immunoprecipitation for DNMT3a will be important to confirm the large photoperiodic variation in DNA methylation and identify the genomic regions targeted in both testicular and uterine tissue. Uncovering the mechanism that underlies this natural pattern could have a significant impact for developing alternative methods for contraceptives. Moreover, these data provide further evidence that epigenetic modifications exhibit dynamic and cyclical patterns in expression and indicate DNA methylation is a key characteristic of timing biological rhythms.

Acknowledgements

This work was funded by the University of Aberdeen CLSM grant to TJS. EWJL was funded by a Society for Reproduction and Fertility undergraduate scholarship. TJS conceived the project, designed experiments, analysed data and wrote the manuscript. EWJL conducted experiments and analysed the data. CC conducted the immunocytochemistry. ML conducted HEK293 cell culture assays. EMC and ASB provided technical assistance. The authors thank Gerald Lincoln for critical feedback on a previous version of this manuscript.

References

1. Stevenson TJ, Ball GF. Information theory and the neuropeptidergic regulation of seasonal reproduction in mammals and birds. Proc Roy Soc B. 2011; 278:2477-2485.

2. Filadelfi AMC, DeLauro Castrucci AM. Comparative aspects of the pineal/melatonin system of poikilothermic vertebrates. J Pineal Res. 1996; 20:175-186.

3. Wood S, Loudon AS. Clocks for all seasons: unwinding the roles and mechanisms of circadian and interval times in the hypothalamus and pituitary. J Endocrinol. 2014; 222:R39-R59.

4. Masri S, Sassone-Corsi P. The circadian clock: a framework linking metabolism, epigenetics and neuronal function. Nat Rev. Neurosci. 2013; 14:69-75.

5. Masri S, Sassone-Corsi P. Plasticity and specificity of the circadian epigenome. Nat. Neurosci. 2010; 13:1324-1329.

6. Azzi A, Dallmann R, Casserly A, Rehrauer H, Patrignani A, Maier B, Kramer A, Brown SA. Circadian behavior is light-reprogrammed by plastic DNA methylation. Nat Neurosci. 2014; 17:377-382.

7. Stevenson TJ, Prendergast BJ. Reversible DNA methylation regulates seasonal photoperiodic time measurement. Proc Natl Acad Sci. 2013; 110:16651-16656.

8. Jones PA, Functions of DNA methylation: islands, start sites, gene bodies and beyond. Nature Rev. Gen. 2012; 13:484-492.

9. Schubeler, D. Function and information content of DNA methylation. Nature 2015; 517:321-326.

10. Marques CJ, Pinho JM, Carvalho F, Bieche I, Barros A, Sousa M. DNA methylation imprinting marks and DNA methyltransferase expression in human spermatogenic cell stages. Epigenetics 2011; 6:1354-1361.

11. Ahluwalia A, Hurteau JA, Bigsby RM, Nephew KP. DNA methylation in ovarian cancer. II. Expression of DNA methyltransferases in ovarian cancer cell lines and normal ovarian epithelial cells. Gynecol Oncol. 2001; 82:299-304.

12. Van Kaam KJ, Delvoux B, Romano A, D'Hooghe T, Dunselman GA, Groothuis PG. Deoxyribonucleic acid methyltransferase and methyl-CpG binding domain proteins in human endometrium and endometriosis. Fertil. Steril. 2011; 95:1421-1427.

13. Roy A, Matzuk MM. Deconstructing mammalian reproduction: using knockouts to define fertility pathways. Reproduction 2006; 131:207-219.

14. Smallwood SA, Kelsey G. De novo DNA methylation: a germ cell perspective. Trends Genetics 2012; 28:33-42.

15. Horton TH, Yellon SM. 2001. Aging, reproduction and the melatonin rhythm in the Siberian hamster. J. Biol Rhythms, 16:243-253.

16. Prendergast BJ, Onishi KG, Patel PN, Stevenson TJ. Circadian arrhythmia dysregulates emotional behaviours in aged Siberian hamsters. Behav. Brain Res. 2014; 261:146-157.

17. Dodge JC, Kristal MB, Badura LL. Male induced estrus synchronization in the female Siberian hamster (Phodopus sungorus). Physiol. Behav. 2002; 77:227-231.

18. Wade GN, Bartness TJ. Effects of photoperiod and gonadectomy on food intake, body weight and body composition in Siberian hamsters. Amer. J Physiol. Reg Integrat Comp. Physiol. 1984; 246:R26-R30.

19. Meisel RL, Luttrell VR. Estradiol increases the dendritic length of ventromedial hypothalamic neurons in female Syrian hamsters. Brain Res Bull. 1990; 25:165-168.

20. Prendergast BJ. MT1 melatonin receptors mediate somatic, behavoral and reproductive neuroendocrine responses to photoperiod and melatonin in Siberian hamsters (Phodopus sungorus). Endocrinol. 2010. 151:714-721.

21. Chen L, He X, Zhang Y, Chen X, Lai X, Shao J, Shi Y, Zhou N. Melatonin receptor type 1 signals to extracellular signal-regulated kinase 1 and 2 via Gi and Gs dually coupled pathways in HEK-203 cells. Biochemistry 2014 53:2827-2839.

22. Zhao S, Fernald RD. Comprehensive algorithm for quantitative real-time polymerase chain reaction. J Comput Bio. 2005; 12:1047-1064.

23. Bustin SA, Benes V, Garson JA, Hellemans J, Huggett J, Kubista M, Mueller R, Nolan T, Pfaffl MW, Shipley GL, Vandesompele J, Wittwer CT. The MIQE guidelines: minimum information for publication of quantitative real-time PCR expreiments. Clin Chem. 2009; 55:611-622.

24. Stevenson TJ, Onishi KG, Bradley SP, Prendergast BJ. Cell-autonomous iodothyronine deiodinase expression mediates seasonal plasticity in immune function. Brain Behav. Immun. 2014; 36:61-70.

25. Banks R, Delibegovic M, Stevenson TJ. Photoperiod- and triiodothyronine-dependent regulation of reproductive neuropeptides, proinflammatory cytokines, and peripheral physiology in Siberian hamsters (*Phodopus sungorus*). J Biol Rhythms 2016: *in press.*

26. West MJ. New stereological methods for counting neurons. Neurobiol. Aging 1993; 14:275-285.

27. Stevenson TJ, Ball GF. Anatomical localization of the effects of reproductive state, castration and social milieu on cells immunoreactive for gonadotropin-releasing hormone 1 in male European starlings. J Comp. Neurol. 2009; 517:146-155.

28. Conway S, Drew JE, Canning SJ, Barrett PJ, Jockers R, Strosberg AD, Guadiola-Lemaitre B, Delagrange P, Morgan PJ. 1997. Identification of Mel1a melatonin receptors in the human embryonic kidney cell line HEK293: evidence of G protein-coupled melatonin receptors which do not mediate the inhibition of stimulated cyclic AMP levels. FEBS Lett. 407:121-126.

29. Stevenson TJ, Visser ME, Arnold W, Barrett P, Biello S, Dawson A, Denlinger DL, Dominoni D, Ebling FJ, Elton S, Evans N, Ferguson HM, Foster RG, Hau M, Haydon DT, Hazlerigg DG, Heideman P, Hopcraft JGC, Jonsson NN, Kronfeld-Schor N, Kumar V, Lincoln GA, MacLeod R, Martin SAM, Martinez-Bakker M, Nelson RJ, Reed T, Robinson JE, Rock D, Schwartz WJ, Steffan-Dewenter I, Tauber E, Thackeray SJ, Umstatter C, Yoshimura T, Helm B. Disrupted seasonal biology impacts health, food security and ecosystems. Proc R Soc B. 2015; 282:1-10.

30. Sasaki H, Matsui Y. Epigenetic events in mammalian germ-cell development: reprogramming and beyond. Nat Rev Genet. 2008; 9:129-140.

31. Kaneda M, Okano M, Hata K, Sado T, Tsujimoto N, Li E, Sasaki H. Essential role for de novo DNA methyltransferase dnmt3a in paternal and maternal imprinting. Nature 2004; 429:900-903.

32. Aoki A, Suetake I, Miyagawa J, Fujio T, Chijiwa T, Sasaki H and Tajima S. Enzymatic properties of de novo-type mouse DNA (cytosine-5) methyltransferases. Nucl Acid Res. 2001; 29:3506-3512.

33. Margolin G, Khil PP, Kim J, Bellani MA, Camerini-Otero RD. Integrated transcriptome analyses of mouse spermatogenesis. BMC Genomics 2014; 15:39

34. Takashima S, Takehashi M, Lee J, Chuma S, Okano M, Hata K, Suetake I, Nakatsuji N, Miyoshi H, Tajima S, Tanaka Y, Toyokuni S, Sasaki H, Kanatsu-Shinohara M, Shinohara T. Abnormal DNA methyltransferase expression in mouse germline stem cells results in spermatogenic defects. Bio. Reprod. 2009; 81:155-164.

35. Maywood ES, Chahad-Ehlers S, Garabette ML, Pritchard C, Underhill P, Greenfield A, Ebling FJ, Akhtar RA, Kyriacou CP, Hastings MH, Reddy AB. Differential testicular gene expression in seasonal fertility. J Biol Rhythms 2009; 24:114-125.

36. Krause A, Krause W. Seasonal variation in human seminal parameters. Eur. J Obstet. Gynecol. Reprod. Biol. 2002; 101:175-178.

37. Levitas E, Lunenfeld E, Weisz n, Friger M, Har-Vardi I. Seasonal variations of human sperm cells among 6455 semen samples: a plausible explanation of a seasonal birth pattern. Am J Obstet Gynecol. 2013; 208:406e1-6.

38. Logan PC, Ponnampalam AP, Steiner M, Mitchell MD. Effect of cyclic AMP and estrogen/progesterone on the transcription of DNA methyltransferase during the decidualization of human endometrial stromal cells. Mol Hum Reprod. 2013; 19:302-312.

Figure Legends

Figure 1 – Photoperiod induced variation in testicular DNA methylation. A) SD significantly reduced testicular mass in males. B) regressed testes were observed to have a robust increase in global DNA methylation. C) the photoperiodic induced change in DNA methylation appears to develop from increased relative expression of *dnmt3a* and to a lesser extent *dnmt3b* (D). Significance is depicted by *** $P<0.001$; ** $P<0.01$; * $P<0.05$.

Figure 2 – Short days increase DNMT3a expression in the testes. A) SD significantly reduced testicular mass. B) the number of DNMT3a expressing cells (summed across 10 seminiferous tubules) in SD regressed testes exhibited a significant increase compared to LD controls. C) and D) exemplar photomicrographs of LD and SD DNMT3a expression in testicular tissue. Note the large decrease in testicular lumen in SD compared to LD samples. White scale bar represents 3mm.

Figure 3 – Ovarian tissue lacks photoperiod-dependent changes in DNA methylation. A) SD hamsters were observed to display a slight decrease in ovarian mass. Unlike the testes, the ovary did not exhibit a significant difference in global DNA methylation (B). Moreover, both *dnmt3a* (C) and *dnmt3b* (D) relative expression remained constant across LD and SD conditions.

Figure 4 – Photoperiod-induced variation in relative *dnmt3a* and *dnmt3b* uterine expression. Female hamsters transferred to SD exhibit a significant decrease in uterine mass (A). SD uterine had significantly more relative *dnmt3a* (B) and *dnmt3b* (C) expression compared to LD controls. Significance is depicted by *** $P<0.001$; ** $P<0.01$; * $P<0.05$.

Figure 5 – Oestrus significantly decreased relative *dnmt3a* expression. A) combined uterine mass and plasma prolactin reliably indicate diestrus (DI), proestrus (PRO) and oestrus phases (EST). Uterine mass is low in diestrus and significantly increased during proestrus and again during oestrus. Plasma prolactin is low in diestrus, significantly increased during proestrus and then decreases during oestrus. B) the levels of relative *dnmt3a* expression are significantly reduced during oestrus. C) there was a non-significant decrease in relative *dnmt3b* expression during oestrus. White, grey and black bars indicate DI, PRO and EST stages respectively. Significance is depicted by *** $P<0.001$; ** $P<0.01$; * $P<0.05$.

Figure 6 – Rapid inhibition of relative *dnmt3a* and *dnmt3b* uterine expression. A) Ovariectomized females treated with a single bolus injection of E2P4 exhibit a significant increase in uterine mass after 24 hrs compared to OIL treated controls. There was a trend for heavier uterine in females after 12hrs. E2P4 injections significantly reduced both relative *dnmt3a* (B) and *dnmt3b* (C) uterine expression. White bars depict OIL, grey bars depict 12hr and black bars depict 24hr treatment groups. Significance is depicted by *** $P<0.001$; * $P<0.05$.

Figure 7 – Melatonin is sufficient to stimulate relative *dnmt3a* and *dnmt3b* expression. HEK293 cells incubated for 4 hours with melatonin exhibited a categorical increase in relative *dnmt3a* (A) and *dnmt3b* (B) expression. Since both *dnmt3a* and *dnmt3b* displayed a stepwise increase and not a dose dependent change in response to increased melatonin, it is likely that melatonin is acting indirectly via other genomic/molecular pathways. Significance is depicted by *** $P<0.001$.

Figure

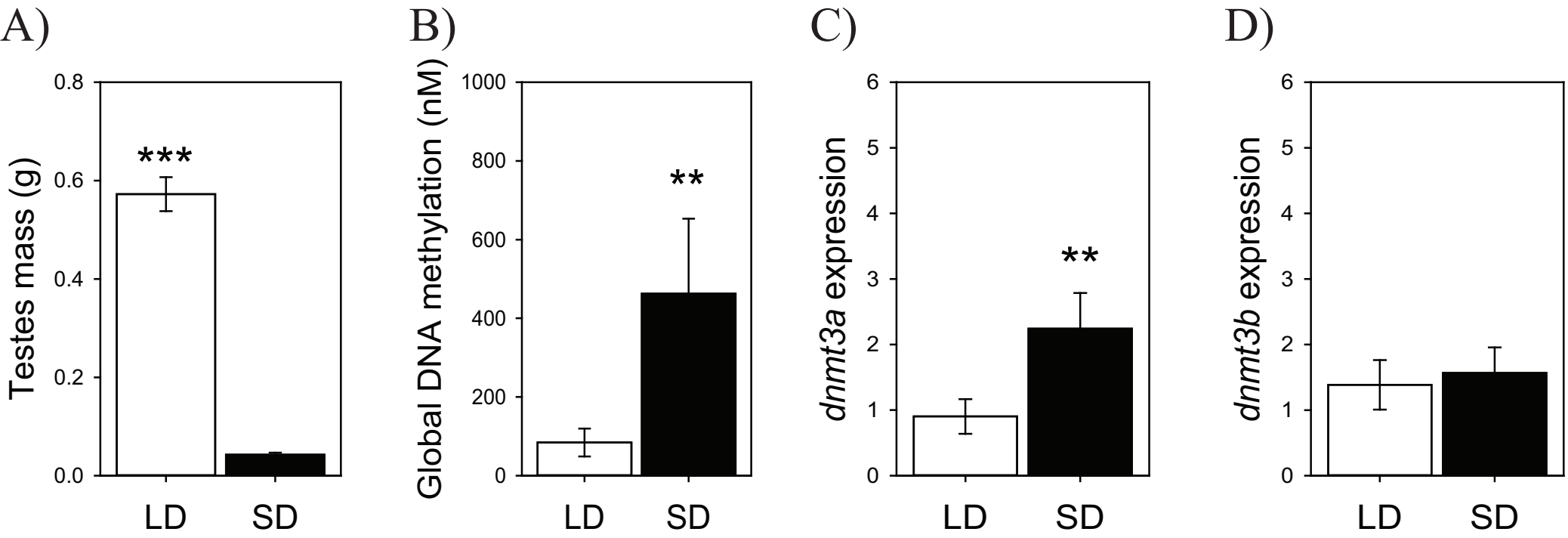
A)
Testes mass (g)
0.8
0.6
0.4
0.2
0.0
***
LD
SD
B)
Global DNA methylation (nM)
1000
800
600
400
200
0
**
LD
SD
C)
dnmt3a expression
6
5
4
3
2
1
0
**
LD
SD
D)
dnmt3b expression
6
5
4
3
2
1
0
LD
SD

Figure

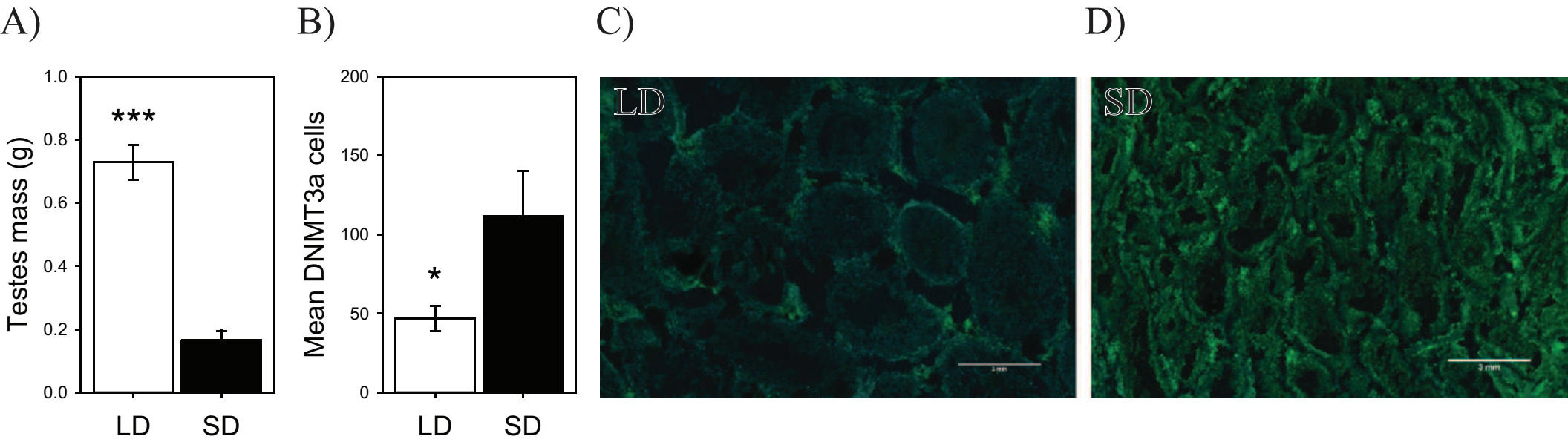
A)
B)
C)
D)
Testes mass (g)
1.0
0.8
0.6
0.4
0.2
0.0
***
LD
SD
Mean DNMT3a cells
200
150
100
50
0
*
LD
SD
LD
SD

Figure

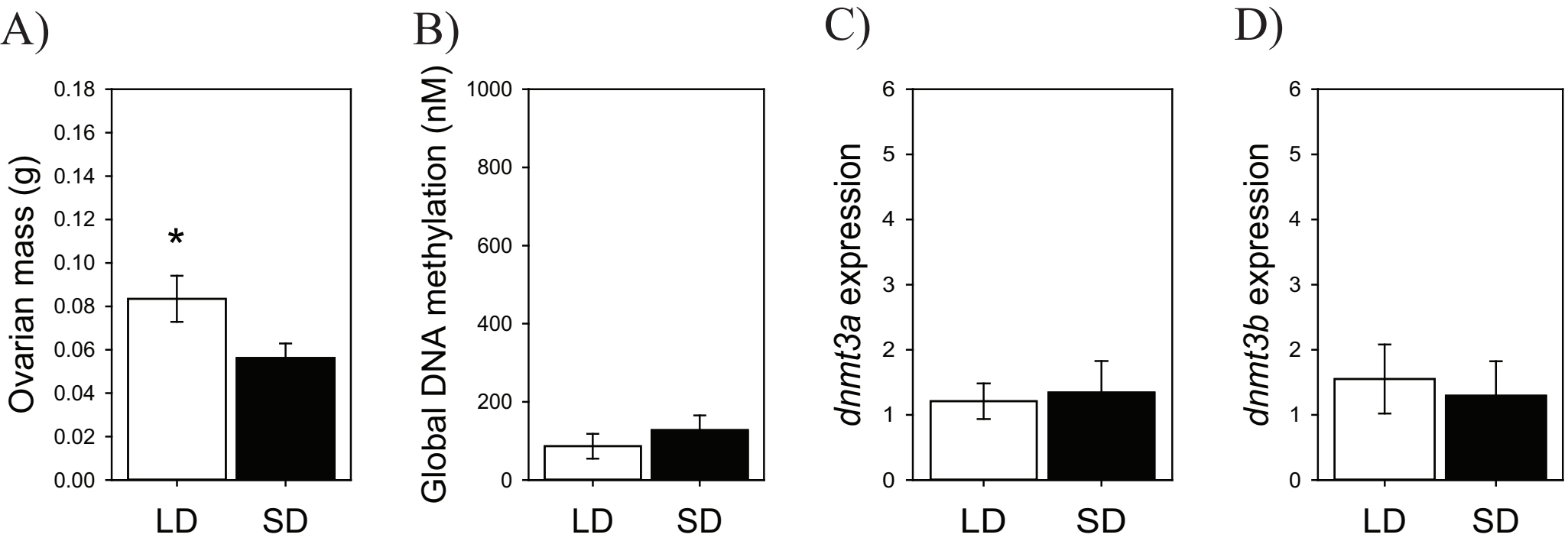
A)
Ovarian mass (g)
0.18
0.16
0.14
0.12
0.10
0.08
0.06
0.04
0.02
0.00
*
LD
SD
B)
Global DNA methylation (nM)
1000
800
600
400
200
0
LD
SD
C)
dnmt3a expression
6
5
4
3
2
1
0
LD
SD
D)
dnmt3b expression
6
5
4
3
2
1
0
LD
SD

Figure

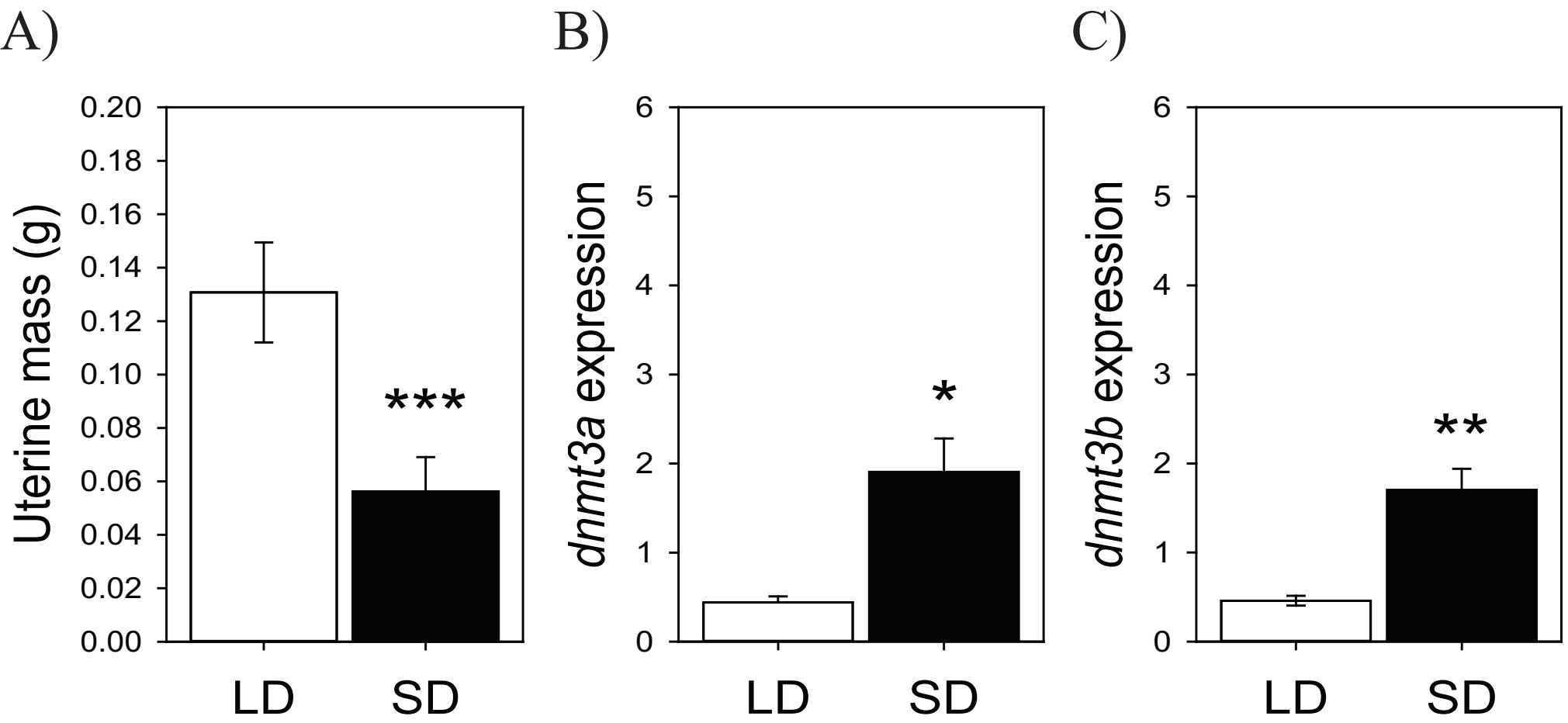
A)
B)
C)
Uterine mass (g)
0.20
0.18
0.16
0.14
0.12
0.10
0.08
0.06
0.04
0.02
0.00
***
LD
SD
dnmt3a expression
6
5
4
3
2
1
0
*
LD
SD
dnmt3b expression
6
5
4
3
2
1
0
**
LD
SD

Figure

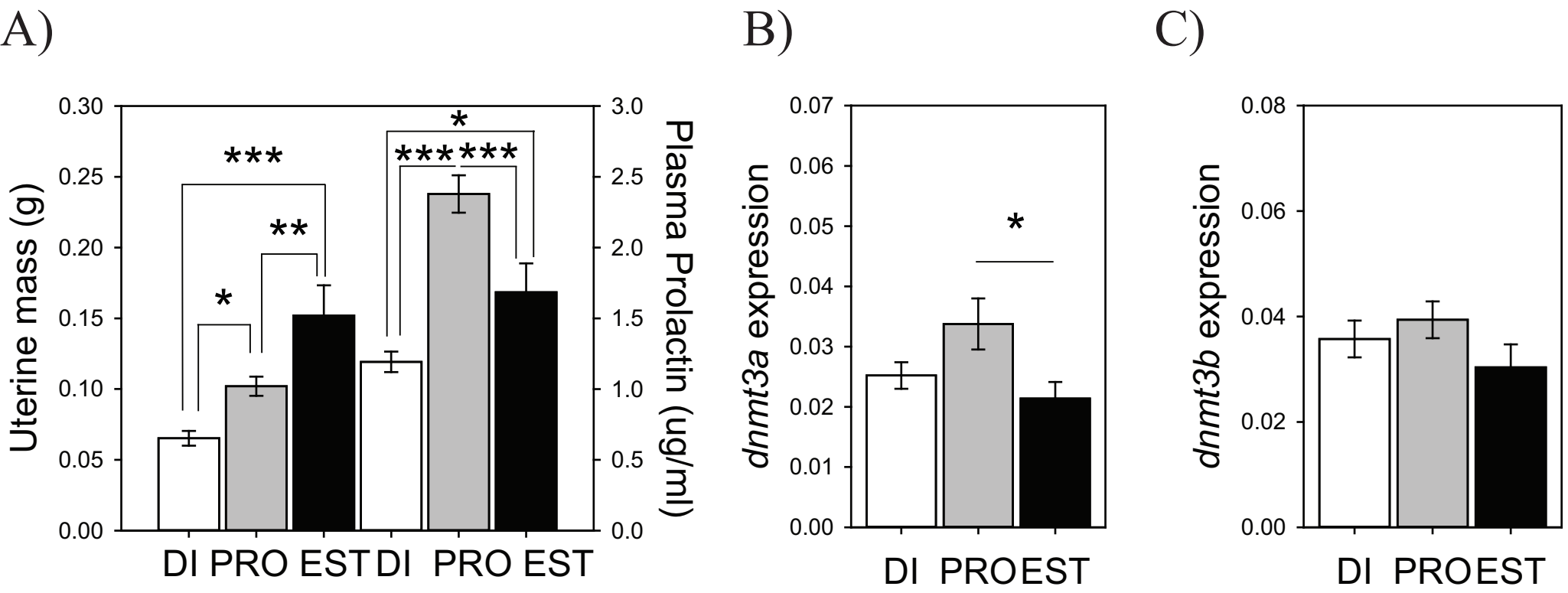
A)
B)
C)
Uterine mass (g)
Plasma Prolactin (ug/ml)
0.30
0.25
0.20
0.15
0.10
0.05
0.00
3.0
2.5
2.0
1.5
1.0
0.5
0.0
***
**
*
*
******
DI PRO EST DI PRO EST
dnmt3a expression
0.07
0.06
0.05
0.04
0.03
0.02
0.01
0.00
*
DI PRO EST
dnmt3b expression
0.08
0.06
0.04
0.02
0.00
DI PRO EST

Figure

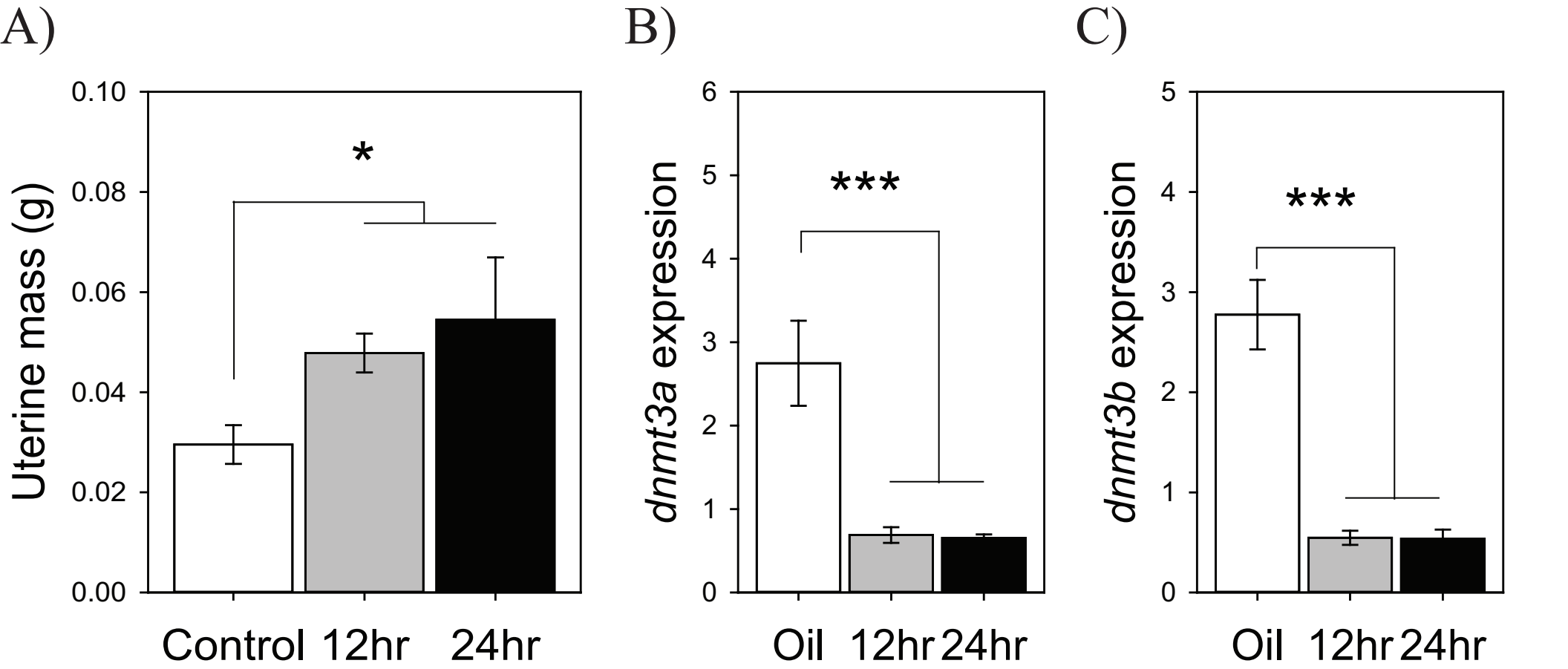
A)
B)
C)
Uterine mass (g)
0.10
0.08
0.06
0.04
0.02
0.00
*
Control
12hr
24hr
dnmt3a expression
6
5
4
3
2
1
0
***
Oil
12hr
24hr
dnmt3b expression
5
4
3
2
1
0
***
Oil
12hr
24hr

Figure

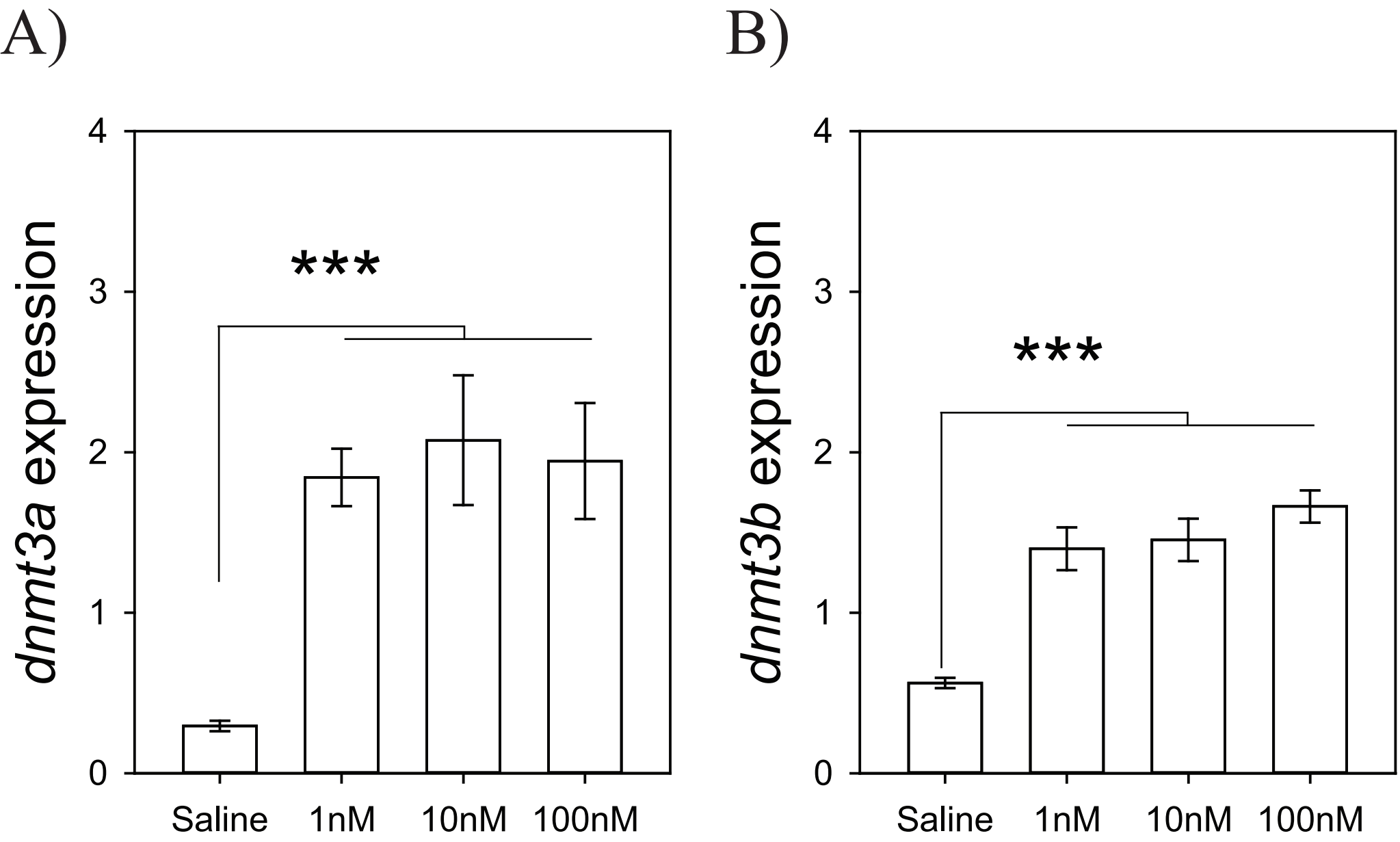
A)
B)
dnmt3a expression
dnmt3b expression
***
***
0
1
2
3
4
Saline
1nM
10nM
100nM

Antibody Table

Peptide/protein target	Antigen sequence (if known)	Name of Antibody	Manufacturer, catalog #, and/or name of individual providing the antibody	Species raised in; monoclonal or polyclonal	Dilution used
DNMT3a	AA 10-118 of human DNMT3a	Anti-DNA Methyltransferase 3a Antibody	ThermoFisher/Invitrogen, PA3-16557	Rabbit polyclonal	1:500